6th IEEE RAS/EMBS International Conference on
Biomedical Robotics and Biomechatronics (BioRob)
June 26-29, 2016. UTown, Singapore

Simplified Robotic Thumb Inspired by Surgical Intervention

Spenser Pulleyking, Dipayan Das, Joshua Schultz, *Senior Member, IEEE*

***Abstract*— Years of empirical trials have refined set angles for the arthrodesis, or surgical fusion, of the metacarpophalangeal joint of the thumb. We capitalize on this knowledge to simplify the design and operation of the thumb throughout a similar range of motion by eliminating a degree of freedom, as inspired by the Steiger arthrodesis. A novel rolling Carpal-Metacarpal joint with magnetic closure is developed that encapsulates abduction/adduction and flexion/extension in the same joint. Thumb workspaces and their volumes were generated from kinematic chain models for different thumb parameters, showing that the prototype's experimental workspace was in agreement with the theoretical model.**

I. INTRODUCTION

In the past few years, the availability of robotic hands and robotic hand designs has dramatically increased. Despite this increase in development, the thumb is still usually treated as another kinematically identical finger that has been attached to the palm at an irregular angle. Though there are notable exceptions [1], no particular kinematic thumb model has become standardized. This also reflects the realization that anatomical functionality among human thumbs is the result of a diverse crowd of kinematic model types [2]. Due to the complexity of the kinematics, some hands [3] rely on the contralateral hand to manually lock the opposing thumb into a series of set positions. The simplification of such "clickable" thumbs does preserve grasping functionality, but does not allow the thumb to circumduct on its own, significantly limiting its independent functionality.

Surgical interventions have, for many years, produced hands that have somewhat reduced functionality but are still highly anthropomorphic, and capable of performing well for everyday tasks. This paper proposes a novel thumb design (shown in Figure 1) that looks to these surgical techniques to balance the anthropomorphic form of the human hand and the functionality and durability of simpler prostheses.

Most mechanical hands fall into one of two classes: anthropomorphic hands that mirror the skeletal, muscular, and kinematic parameters of the human hand [4], and non-anthropomorphic designs that do not resemble human hands [5] [6]. The former has much to offer to future robotic hand designs as an accurate model of human manipulation. The latter represents the most functional robotic hands in industry today, yet is structurally based on the same claw-like mechanics which have been available in prostheses for nearly a century [7] [8]. Pinch grip manipulators preserve very little of the hand's anthropomorphic functionality, but are still more practical than anatomically accurate manipulators.

All authors are with the Department of Mechanical Engineering, the University of Tulsa, Tulsa, OK 74104, USA. Research supported by NSF NRI 1427250 and the Tulsa Undergraduate Research Challenge
joshua-schultz@utulsa.edu

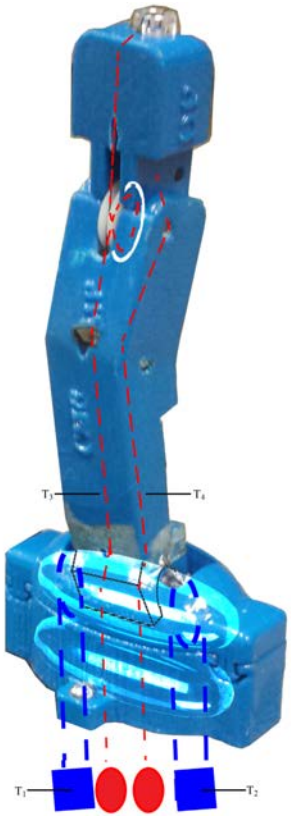

Fig. 1. Photograph of the prototype model. This prototype is based on the proposed Steiger arthrodesis at the MP joint of the thumb, and also on the proposed CMC ellipsoidal joint.

The ACT hand is a very complex, biologically functioning hand model [4]. It is intended to study hand kinematics and biological function rather than serve as an end effector for doing tasks. Bowstringing, or the tendon traveling through free space, causes the ACT thumb's tendons to pull away from the digit as it comes under tension. Though it mimics human movement well, the tendons are exposed and interfere with the environment.

Many mechanical features in biology arise from factors other than manipulative processes, such as the need for all structures to be built by cell regeneration. The biological hand is very adept at coping with mechanical damage: after surgical simplification, patients who have lost range of motion can still perform most tasks. A compromise can be made between the complicated nature of anthropomorphic design and the functionality of simplified kinematics, known surgically as arthrodesis: a procedure that simplifies a joint

978-1-5090-3287-7/16/$31.00 ©2016 IEEE

TABLE I

MAIN TENDONS OF THE THUMB SIMPLIFIED FROM 8 TO 4

Natural Tendon	Function	Replaced By
Abd. Pollicis Longus	CMC Add.	T_1
Abd. Pollicis Brevis	CMC Abd.	T_2
Ext. Dorsal Expansion	MP Add./Abd., IP Ext.	T_3
Ext. Pollicis Brevis	CMC Add.	T_1
Oppenens Pollicis	CMC/IP Flex.	T_4
Add. Pollicis	CMC Abd.	T_2
Ext. Pollicis Longus	CMC/MP Ext.	T_3
CMC Joint Capsule	Joint Stability	Sliding Cap

by fusing it at a permanent set of angles [9].

Through the empirical process of many trials over many years, surgeons have refined set angles of fusion that they deemed best for a metacarpophalangeal (MP) thumb joint arthrodesis. We explore this knowledge to develop a simplified thumb. Guided by the surgical compromise of the arthrodesis, the carpometacarpal (CMC) and the MP joint may be greatly simplified in implementation. Inspired by this surgical implementation, the robotic thumb in this work eliminates the MP in a similar fashion, likewise preserving the majority of the workspace. It also develops a novel prolate CMC joint that provides flexion-extension and abduction-adduction of the thumb in the same joint.

II. CONSIDERATION OF BIOLOGICAL END EFFECTORS

The biological thumb needs to be able to rotate in order to position the pulp in the proper orientation. As the thumb adducts or abducts at the CMC and MP joints, these joints also rotate the thumb itself. The purpose of this is to ensure that the pulp of the thumb tip is always suitably oriented with regard to the grasped object, since the distal phalanx must also accommodate the spatial needs of fingernails. This rotational coupling is a result of two other types of motion that are codependent in the thumb: pronation and supination [10]. This is significant to functionality, because the pulp of the thumb is its biological end effector. Chalon [11] intentionally mis-aligns the axis of the MP and interphalangeal (IP) joints with those of the CMC, so that the thumb rotates as it flexes, just like a human thumb. If the pulp did not rotate via pronation, grasping would be very difficult and unstable.

This instability is based on the assumption that the orientation of the pulp of the thumb tip is restricted by the limited range of motion of the IP joint, at 110° [12]. By eliminating the nail and freeing up that space, the pulp can wrap completely around the distal phalanx in a robotic hand, such that it will be ready to act at any location in the workspace at any degree of flexion, extension, abduction or adduction; thus rotation can be eliminated in a robotic thumb.

The joint most distal from the base of the thumb, the IP, has only one Degree of Freedom. The normative limit of IP extension is not easily defined, as there is a large and continuous spectrum of IP extension limits among the population, with the most extreme case being known as the *Hitchiker's Thumb* [13] [14]. Since this extreme range of motion is not required for grasping purposes, it is not preserved. Our prototype's IP joint remains fundamentally unmodified from its biological equivalent, with an average joint range of 0° to 80° [12]. The MP and CMC joints of the human hand fill much more complex roles in grasping and manipulation than the IP, but their importance is preserved even if they cannot both flex individually. In nature, each of these joints utilizes a series of sliding joints that cannot be easily replicated in a mechanical way. By simplifying the mechanics of these joints we can create a repeatable manufacturing process with acceptable losses in kinematic accuracy.

TABLE II

VOLUMES OF ALTERNATIVE THUMB WORKSPACES

Model Parameters	Volume (cm^3)	% reduction
Unfused	504.2	
Steiger	207.1	58.9%
Wheeless	223.5	55.7%
Prototype (Steiger)	241.0	52.2%

III. ARTHRODESIS OF THE MP JOINT

From a robotics perspective, the preservation of an end effector's workspace is crucial to its function. In the field of orthopedic surgery, this problem has been recognized for many years. Arthritis, carpal tunnel, and other serious forms of degeneration are very common to the thumb joints, and often require reducing their range of motion. Surgeons have found that fusion of the MP joint both alleviates pain and preserves good hand functionality, whereas fusion of the CMC or IP has more adverse affects [9].

Arthrodesis is a well known procedure intended to repurpose a joint using fusion. The damaged joint is fused with a series of metal screws and plates that permanently lock the joint at a specific set of angles. Robotics methodology is useful to explore the volume of the thumb's workspace after such a treatment, relative to the volume of the natural thumb's workspace. This is useful to identify the reduction in workspace posed by arthrodesis on a robotic thumb manipulator.

Two sets of angle parameters have emerged from these trials, specifically for the arthrodesis of the thumb's MP joint. The first model, proposed by Steiger, suggests that the MP joint be reduced from 2 Degrees of Freedom (DoF) to 0 DoF, a total fusion at 10° of flexion and 15° of abduction. Alternatively, the second model, proposed by Wheeless, suggests that the MP joint be allowed to retain motion about 1 DoF: thus, a limited range of 10° to 20° flexion, and a fixed angle of 20° abduction [15] [16].

To evaluate which arthrodesis parameters work better for an anthropomorphic hand, the volume and shaping of their resultant thumb workspaces can be overlaid in the same 3D space, and visually inspected by comparing it to an identical but unfused thumb's workspace, as seen in Figure 2. To generate these workspaces, Denavit Hartenberg Parameters (DH) shown in Table III were used to develop the thumb forward kinematics [17].

To simulate the workspace volume, a function was written using *Mathematica 10.1* to send various discrete joint angles

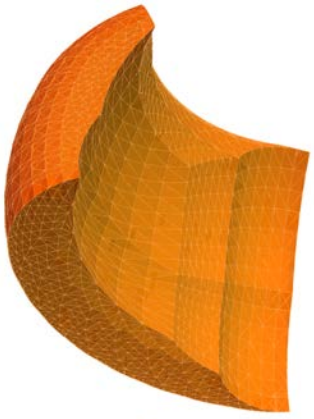

(a) Unfused workspace

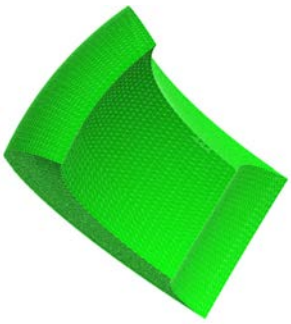

(b) Steiger workspace

(c) Wheeless workspace

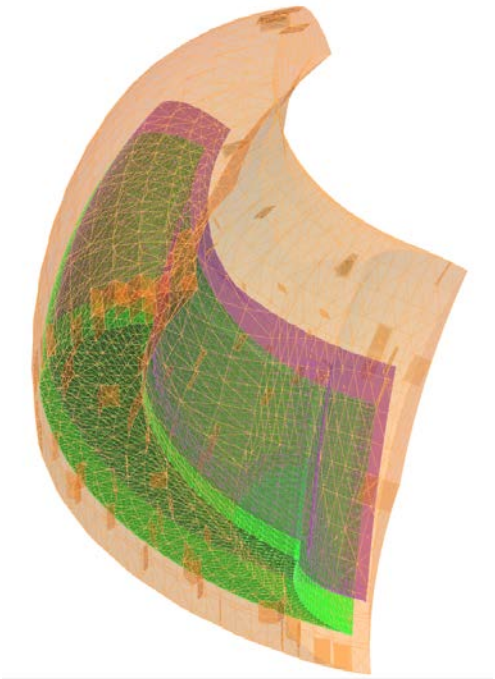

(d) Unfused, Wheeless and Steiger Workspaces

Fig. 2. Workspaces of a left handed thumb. The effect of the arthrodesis is seen immediately between (a) and (b), as (b) has around half the size of the unfused volume. Steiger's and Wheeless' parameters produce similarly shaped point clouds, with the main variation being the positioning within the unfused cloud. The Steiger fusion results in a marginally smaller volume than the Wheeless fusion; both fusions are about half the volume of the unfused workspace. The lost portion of the workspace due to the interventions is the portion which positions the thumb closest to the palm of the hand, which is seldom used in tasks of everyday living.

through the series of transformation matrices calculated for each joint, which predict the resultant end effector location. This resulted in a series of points in 3D task space, which corresponds to the thumb's overall range of motion. For both fusions and the unfused workspace, 3D point clouds were generated, representing the 3D workspace volume of each thumb model as shown in Figure 2.

Because the Wheeless workspace's 1 DoF retains the complexity of articulating the MP joint, without increasing the volume of the workspace over the Steiger, the Steiger arthrodesis was selected as the basis of the robotic thumb design (seen in Table II). The DH parameters of all workspace models are shown in Table III. d_i=0 is true for all joints, meaning the links are not offset from one another along the z_i axis. Link lengths ℓ are defined at the bottom of Table III. The symbol – in Table III denotes the range between the two extreme angle values that was discretized to generate joint values. While a_{i-1} is usually a constant, the changing displacement of the point of contact from the centroids requires that the term be treated as a function of θ_2, as explained in subsection VI-A.

IV. Tendon Routing Simplification

The thumb prototype utilizes a tendon and pulley system instead of localized actuators, as in [18], [11], and [4]. This further minimizes the complexity of the device by having as few actuators as possible. This improves durability, reducing weight and cost, and is more biologically inspired.

The thumb has a large number of tendons that actuate it, but as many of these are attached to thenar muscles with small cross sections, their tendons can be combined with those of the larger muscles and only the most subtle motions of the thumb are lost. Tendons which are used primarily for thumb manipulation are shown in Table I [19]. As can be seen in Figure 1, our prototype thumb simplifies its tendon network into 4 tendons: one each for adduction, abduction, flexion, and extension. Having four tendons arranged in this symmetric way allows for easy coordinate control and input.

The locations of the IP joint and the ellipsoids of the CMC joint are highlighted in white and blue, respectively. The blue squares at the bottom represent single tendons that split around the ellipsoids and terminate at the base of the metacarpal. From right to left, the blue tendons control adduction and abduction, respectively. The red tendons control flexion and extension, and terminate in the distal phalanx. To allow for underactuated grasping, the motion of the IP joint is mechanically coupled with that of the CMC joint via the flexor and extensor tendons.

In theory, one could simplify the tendons further: by coupling the hybrid extensor tendon T_3 with T_1 and T_2, then allowing that hybrid extensor tendon to also be coupled to the IP joint's extension, the two adduction/abduction tendons can be migrated to the extensor side. Distributing T_3's load among T_1 and T_2, T_3 is eliminated and a tripodal stability becomes possible, though harder to control. Also, this makes operation of the IP joint (when it is also under adduction or abduction) much more difficult, as the tendons must work

TABLE III

DH PARAMETERS FOR TRANSFORMATION MATRICES M_i.

Input Variable (IV)	α_{i-1}	a_{i-1}	θ_i
Computational Order:	1	2	3
Units:	(deg.)	(mm)	(deg.)
IV Function:	Rot. x_{i-1} axis	Tran. x_{i-1} axis	Rot. z_i axis
Unfused M1	0	0	0–70
Unfused M2	90	0	-15–20
Unfused M3	0	ℓ_{mcp}	-15–15
Unfused M4	-90	0	0–50
Unfused M5	0	ℓ_{pp}	0–80
Unfused M6	0	ℓ_{dp}	0
Steiger M1	0	0	0–70
Steiger M2	90	0	-15–20
Steiger M3	0	ℓ_{mcp}	10
Steiger M4	-90	0	15
Steiger M5	0	ℓ_{pp}	0–80
Steiger M6	0	ℓ_{dp}	0
Wheeless M1	0	0	0–70
Wheeless M2	90	0	-15–20
Wheeless M3	0	ℓ_{mcp}	20
Wheeless M4	-90	0	10–20
Wheeless M5	0	ℓ_{pp}	0–80
Wheeless M6	0	ℓ_{dp}	0
Prototype M1	0	0	-12.5–12.5
Prototype M2	90	0	-4.375–4.375
Prototype M3	0	F(θ_2)	G(θ_2)
Prototype M4	0	F(θ_2)	θ_2
Prototype M5	-90	ℓ_{mcp}	θ_1
Prototype M6	90	0	10
Prototype M7	-90	ℓ_{pp}	15
Prototype M8	0	0	-11–107.5
Prototype M9	0	ℓ_{dp}	0

Structure	Variable	Length (mm)
Metacarpal	ℓ_{mcp}	52.9
Proximal Phalanx	ℓ_{pp}	40.3
Distal Phalanx	ℓ_{dp}	30.7
Ellipsoid Major Radii	R_{maj}	21.02
Ellipsoid Minor Radii	R_{maj}	7.60

against each other. Cocontraction would significantly limit the grip strength of the thumb, while 4 tendons allow for much more efficient energy transmission during grasping, due to the radial location of each tendon with respect to the ellipsoids. This is why the four-tendon simplification was chosen.

V. CMC JOINT: TWIN PROLATE ELLIPSOIDS

A. Mechanical Design Justification

Mechanical Thumbs often use a pin joint, two pin joints coupled at perpendicular axes of rotation, or simply a joint with a series of locking positions to approximate the function of the CMC joint [5] [1] [3]. The CMC joint described in this paper uses ellipsoidal magnets to approximate the conic rolling path taken by the natural thumb's metacarpal across its trapezium. The purpose of the magnetism is to bind the ellipsoids together as the joint moves, as their dependent polar attractions restore the ellipsoids' precise alignment when the joint returns to its resting position, defined by the alignment of both ellipsoids with the length of the metacarpal.

The range of motion of the CMC has been defined many different ways, with significant disagreement on how to characterize the rolling of the metacarpal across the highly irregular surface of the trapezium [20]. The CMC does not fit neatly into a Reuleaux kinematic pair, not does it lend itself easily to being reduced to a system of traditional joints. Rather, it is best modeled as a complex surface joint [21]. Chalon, et. al. [11] suggests the use of an ellipsoidal surface joint as the best way to mimic the rolling/gliding motion of the CMC joint complex.

To accommodate this joint's large range of motion, mechanical limits were established by creating an encasement around the CMC joint. The joint occurs at the mutual contact point of the two ellipsoids, in the middle of the joint housing. This encasement, called the sliding cap, has a central opening for the metacarpal, with rectangular surfaces parallel to the outer faces of the metacarpal, which prevents metacarpal rotation about the contact point between the ellipsoids. As shown in the companion video, the sliding cap performs three functions: first, it limits the range of motion in flexion-extension and abduction-adduction. Second, it prevents large rotations about the contact point. Third, it prevents grasping forces from forcing the magnetic joint apart. In addition to these functions, the durability of the joint is improved by the cap's force-limiting breakaway feature shown in Figure 4.

After the structural components were 3D printed using ABS plastic, vaporized acetone was used to dissolve their outermost layers. Using short exposures, this removes the ridges from the rapid prototyping process, resulting in a low-friction finished surface that improves the sliding action of the CMC joint's sliding cap. The sliding surfaces of the cap are also lubricated using graphite powder to further prevent jamming. Alternatively, using long exposures to the vapor, the tip of the thumb is given a 'softened' surface which is also finished, but with higher surface friction due to the dissolution and restructuring of more of the thumb's outer layers; this improves the gripping capability of the distal phalanx.

B. Choice of Ellipsoids

Ellipsoids, as do spheroids, share a fundamental property: when one is rolling about another, it rotates along its own axis twice as rapidly, in terms of angular deflection from the vertical resting position. This means the metacarpal needs to roll only half as far as it would on a flat surface to generate an equivalent amount of rotation. This doubling results in a significant decrease in the overall size of the joint housing. Thus, twin ellipsoids seem to be a compact way to use the concept for a thumb joint.

Our design used a pair of ellipsoids manufactured by Westminster Inc. known as Rattlesnake Eggs™. These ellipsoids have the required surface and magnetic strength, though they are not perfectly ellipsoidal. They are powerful magnets whose magnetic poles run perpendicular to their major axis, so they are most stable magnetically when side by side, as shown in Figure 3. The chosen ellipsoids are also prolate, which allows for greater range of motion when the trajectory is along the minor radii of the ellipsoids. Thus, as shown in Figure 1, the minor radial discs of the ellipsoids are coplanar

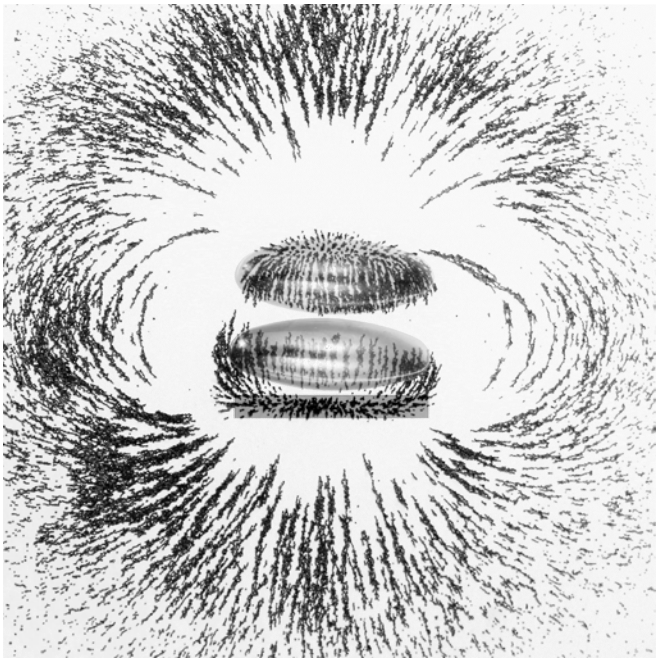

Fig. 3. Iron filings show the magnetic field in the CMC joint. The effect of the ferrous plate is seen in the stacked filings directly below the bottom elipsoid, with which the plate is in direct contact. These stacked filings represent the magnetic field lines, which emerge from the page along the plane of the ferrous plate.

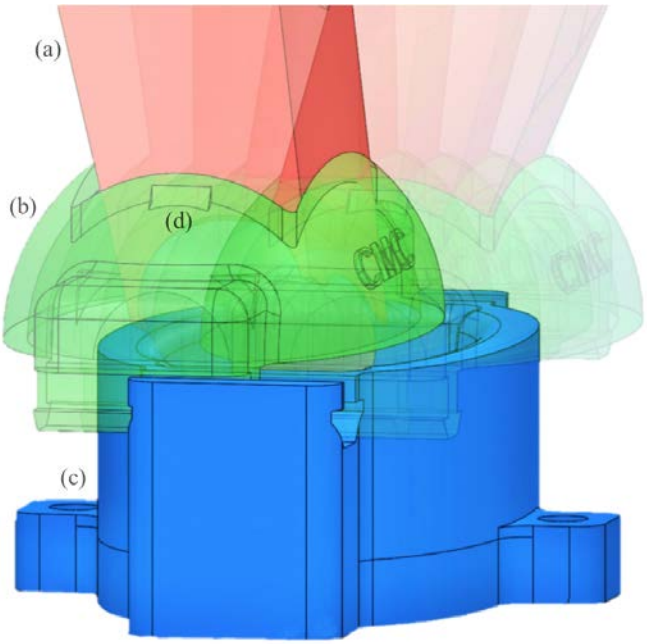

Fig. 4. This CAD representation shows the CMC joint following a trajectory across both ranges of motion at once. The bottom of the CMC joint (c) is approximately coplanar with the plane of the palm of the hand. The metacarpal-interphalanx fusion (a) is prevented from twisting about its own axis by the CMC cap (b), but can dislocate in emergencies due to the breakaway feature (d), preventing structural damage.

with the flexion/extension axis of the metacarpal. The major axis of the ellipsoids is perpendicular to this, inhabiting the plane of CMC adduction/abduction motion.

C. CMC Joint Limits: Magnetic and Mechanical

To enforce the CMC joint limits, one of the ellipsoids is inserted into the bottom of the ABS joint housing, and secured in place with a small elliptical plate of steel. This plate is ferrous, and interacts in a beneficial way with the ellipsoids, creating a third point of attraction directly below the first two. This ensures that the ellipsoids' magnetic poles point straight upwards from the plate.

As the steel plate also defines the base plane of the thumb's first reference frame, the most stable point for the finger is in alignment with the base's normal vector (when the ellipsoids' poles are parallel) as shown in Figure 3. The magnetic forces causing this effect can be seen in the linear concentration of iron filings along the plane of the plate. These magnetic joint forces cause the thumb to return to the same resting orientation, even if the ellipsoids' point of contact has been rotated or shifted without rolling. Magnetic interaction also creates partial joint forces to help hold the thumb together passively, so that under extreme duress it can come free without structural failure, but under normal usage will not jam or become misaligned.

D. Prototype Durability

The second ellipsoid is secured to the metacarpal with an adhesive. When the CMC is in resting position, the metacarpal is parallel to the ellipsoid's major axis and collinear with the magnetic poles aligned below it. As part of the metacarpal, the top ellipsoid will rotate around and over the base ellipsoid, which remains fixed. This motion is meant to closely mimic that of a natural CMC joint. The sliding cap has 1 DoF, and travels over the ellipsoids as seen in Figure 4. If a directional load is powerful enough to overcome the magnetic forces and mechanical limits, the breakaway feature will allow the thumb to dislocate at the CMC, before any structural damage can occur. This designates the thumb as a known weak point, eliminating the need for breakaway features in the other fingers of the hand during grasping, and expediting any necessary repairs.

E. CMC Tendon Routing

As seen in Figure 1, flexion/extension of the CMC is coupled to the IP joint, to allow underactuated grasping motions, such as those envisioned for the underactuated TU Hand [18]. Abduction/Adduction tendons travel through holes in the plate and base, then terminate within the CMC joint, respectively secured to the mobile ellipsoid's prolate poles. These tendons do not need to extend further along the finger, as the MP fusion means that there is no need for abduction/adduction further down the digit, as shown in Figure 1. This early termination allows the tendons to remain within the structure of the thumb itself, as it prevents bowstringing, an issue observed in tendon-driven mechanical thumb models. The danger of a finger's tendon bowstringing

is greatest in the thumb's MP joint: its unique kinematic requirements mean that its abduction-adduction tendons are joined to the palm far from the base of the thumb, as shown in [4]. The remaining two tendons travel up to the distal phalanx, coupling IP and CMC flexion/extension.

VI. Evaluation of Thumb Workspace

A. CMC Ellipsoid Joint Workspace Simulation

In Table III, the DH parameters used for the calculation of the prototype's workspace are defined, which are used with the joint limits to compute the workspace. As the CMC joint does not represent a constant link length or angle, new forward kinematics functions were developed to step through the joint using virtual linkages. Starting from the base of the CMC, the first and second linkages mirror each other about the tangent plane shared by the ellipsoids at their point of contact. The first linkage travels from the centroid of the base ellipsoid to the point of contact between the two ellipsoids, and the second linkage travels from this point of contact to the centroid of the mobile upper ellipsoid.

As these linkages' equivalent magnitudes are always changing over the abduction/adduction of the CMC, they are defined by the radial distance from the center of the ellipsoid to its surface, which can be represented by a function of θ_1, θ_2, and the ellipsoids' major and minor radii, respectively R_{maj} and R_{min}. This function is represented by $F(\theta_2)$ in equation (1). The internal angle between these two linkages at the junction is determined as a function of the slope of the tangent plane of the ellipsoid, represented by $G(\theta_2)$ in equation (2). In Table III, these functions are used to determine the forward kinematics of the variable-length linkages within the CMC, which are presented in Figure 5. As described in subsection V-B, rotation of one ellipsoid around another doubles the change in the joint angle, which is why θ_1 and θ_2 are respectively reused for θ_4 and θ_5 in Table III. From the base of the metacarpal to the end effector, the DH parameters are subsequently identical to those of the Steiger arthrodesis.

$$F(\theta_2) = \left| \sqrt{R_{maj}^2 / (1 - \cos^2\theta_2 + \left(\frac{R_{min}}{R_{maj}}\right)^2 \cos^2\theta_2)} \right| \quad (1)$$

$$G(\theta_2) = 2(\tan^{-1}(\left(\frac{R_{min}}{R_{maj}}\right)^2 \tan|\theta_2|) - |\theta_2|)\sin(-\theta_2) \quad (2)$$

This method of virtual linkages, while effective at predicting the final positions of the links, misses some of the kinematic subtlety of the rolling contact. In reality, the rolling contact is defined at the velocity level. Replacing constraints such as these with a redundant set of position-level constraints (as we have done here) is commonly performed [22], but it is not immediately clear whether this rolling constraint is integratable (and therefore holonomic), or nonholonomic. This will be modeled more rigorously in future work, using workspace modeling based on the Bolzmann-Hamel equations [23]. Physically speaking, the rotational limits imposed by the sliding cap on the metacarpal make the possibility that the thumb could migrate to another spot (a consequence of nonholonomy) highly unlikely; the magnetic field also helps the thumb return to its preferred position.

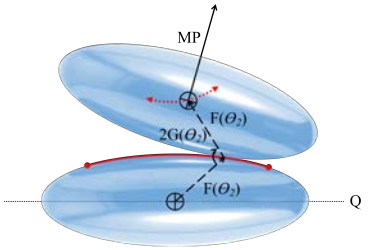

Fig. 5. The ellipsoids, shown in blue, here demonstrate the rolling kinematics of the CMC joint for abduction/adduction only. The solid red curve represents the contact points between the two ellipsoids; if flexion/extension were shown, the curve would become an area on the surface of the lower ellipsoid. The virtual linkages, shown as dashed vectors, are of equal length $F(\theta_2)$ and begin at the centroid of the fixed ellipsoid. They form the interior angle $2G(\theta_2)$. The dotted red curve defines the mobile ellipsoid's centroid, and the solid vector shows the real MP linkage which follows the virtual linkages. Rolling kinematic motion including flexion/extension are similar, where the contact point can roll about axis Q.

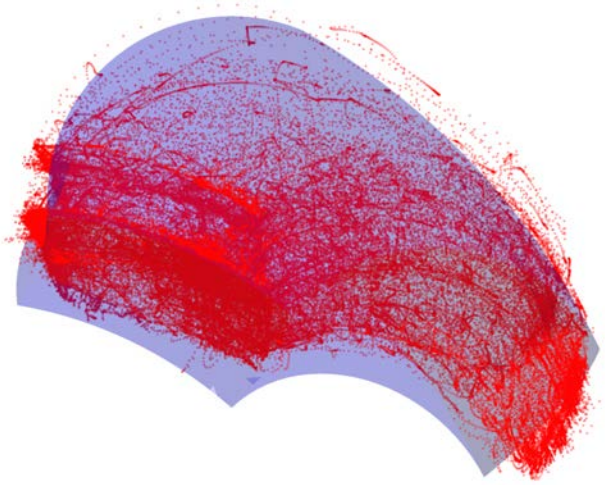

Fig. 6. The red points were recorded from the prototype's motion capture data and plotted simultaneously with the theoretical workspace of the prototype, which was generated using the Steiger model. This theoretical workspace appears as a blue volume, and is similar to the workspace shown in Figure 2b, but its calculation also incorporates the kinematics of the prolate ellipsoids shown in Figure 5.

B. Experimental Results

Using the Polhemus Liberty electromagnetic motion capture system, the location in $\mathbb{R}^3$ of the tip of the thumb was measured, as the tendons were pulled manually from below the base of the thumb. 10 trials were run over a period of 1 minute each, generating 143,796 data points. This point cloud data is shown in Figure 6, and was gathered at a rate of 240 Hz. After duplicate points were removed, the point cloud was compared with the theoretical workspace.

The simulated workspace agrees with the experimental data, suggesting that the transformations are describing the

prototype accurately. The data shows that the prototype is able to reach nearly all locations in the Steiger workspace by suitable manipulation of the tendons. A better metric of this would be to measure the volume of the point cloud, but due to the number of internal points, there is no general algorithm for the extraction of a valid surface. Other methods may prove more successful: for future research, a voxel-based binning method as employed by Bullock and Dollar [24] may produce better results.

One of the major limitations of the prototype is that the sliding cap's mechanical joint limits imposed some restrictions along some ranges of motion. The CMC flexion/extension range was reduced from the theoretical model's range of 70° to 52°, a decrease of 26%. The adduction/adduction range was more accurate, allowing 38° instead of 35°, an increase of 9%. On the other end of the spectrum, the prototype's IP joint is hyper flexible (most likely due to the ABS deforming from frequent use) with a range of -11° to 107°, representing a 47% increase. Yet, this is not outside normal IP joint range for many individuals.

Occasional jamming of the CMC sliding cap was observed to occur as the thumb was brought from full extension to full flexion, causing the thumb to exclude some of its workspace. This can be addressed by finding a better lubricant for the sliding joint, or using a manufacturing material less prone to flexing and jamming, which was the main downside of using ABS.

The success of Steiger's arthrodesis in the surgical world suggests that the workspace generated by his parameters provides sufficient thumb functionality for the activities of daily living. The workspace volume of the prototype, shown in Table II, exceeds the Steiger workspace's volume by 16.4%, and the Wheeless's workspace volume by 7.8%. When looking at volume and shape as indicators of workspace functionality, the prototype exceeds Steiger's volume, though it is of a slightly compressed shape due to the narrowed range limits of the CMC.

VII. CONCLUSIONS

Two novel biologically inspired simplifications to an anthropomorphic robotic thumb were explored: A joint fusion inspired by the Steiger arthrodesis, eliminating the need for an articulated MP joint, and a rolling CMC joint capable of abduction-adduction and flexion-extension. Based on these simplifications, a prototype thumb was developed that focuses on maximizing durability and functionality, while minimizing cost and complexity. The workspace volume of the Steiger-inspired prototype was the largest of all the joint fusions analyzed by the kinematic models, whose accuracy was demonstrated using motion-capture technology.

Future work will improve the design of the prototype by increasing the accuracy of its ranges of motion, improve the design's overall compactness and durability by investigating new materials and tendon routings, and refine its workspace analysis by exploring different methods of kinematic modeling. A more rigorous analytical model for the rolling constraint of the CMC joint will also be developed. By incorporating these changes into a refined prototype, our thumb's functionality will be tested using grasping experiments in an underactuated anthropomorphic five-fingered hand.

REFERENCES

[1] G. Palli, C. Melchiorri, G. Vassura, U. Scarcia, L. Moriello, G. Berselli, a. Cavallo, G. De Maria, C. Natale, S. Pirozzi, C. May, F. Ficuciello, and B. Siciliano, "The DEXMART hand: Mechatronic design and experimental evaluation of synergy-based control for human-like grasping," *The International Journal of Robotics Research*, vol. 33, no. 5, pp. 799–824, 2014.

[2] V. J. Santos and F. J. Valero-Cuevas, "Reported anatomical variability naturally leads to multimodal distributions of Denavit-Hartenberg parameters for the human thumb," *Transaction on Biomedical Engineering*, vol. 53, no. 2, pp. 155–63, 2006.

[3] R. L. Steeper, "The Hand," 2015. [Online]. Available: http://bebionic.com/the_hand

[4] L. Y. Chang and Y. Matsuoka, "A kinematic thumb model for the ACT hand," *Proceedings - IEEE International Conference on Robotics and Automation*, vol. 2006, no. May, pp. 1000–1005, 2006.

[5] B. Townsend, "Barrett Hand," 2015. [Online]. Available: http://barrett.com/products-hand.htm

[6] O. Brock, A. Fagg, R. Grupen, R. Platt, M. Rosenstein, and J. Sweeney, "A Framework for Learning and Control in Intelligent Humanoid Robots," *International Journal of Humanoid Robotics*, vol. 2, no. 3, pp. 301–336, 2005.

[7] R. Bowers, "Prosthetic Devices for Upper-Extremity Amputees," *Amputee Coalition*, 2005.

[8] K. Hawkins, "How easy is it for the limbless to get a bionic arm or leg?" *BBC News*, 2015.

[9] S. W. Wiesel, *Operative Techniques in Hand, Wrist, and Forearm Surgery*. Lippincott Williams & Wilkins, 2010.

[10] M. J. Barakat, J. Field, and J. Taylor, "The range of movement of the thumb." *Hand (New York, N.Y.)*, vol. 8, no. 2, pp. 179–82, 2013.

[11] M. Chalon, M. Grebenstein, T. Wimböck, and G. Hirzinger, "The thumb: Guidelines for a robotic design," *IEEE/RSJ 2010 International Conference on Intelligent Robots and Systems, IROS 2010 - Conference Proceedings*, pp. 5886–5893, 2010.

[12] W. B. Greene and J. D. Heckman, *The Clinical Measurement of Joint Motion*. American Academy of Orthopaedic Surgeons, 1994.

[13] B. Glass and J. Kistler, "Distal hyper-extensibility of the thumbs." *Acta Genet Stat Med*, vol. 4, no. 2-3, pp. 192–206, 1953.

[14] J. H. McDonald, "Hitchhiker's thumb: The myth," *Myths of Human Genetics*, 2011.

[15] V. R. Steiger, "Arthrodesis of the metacarpophalangeal joint of the thumb." *Handchirurgie, Mikrochirurgie, plastische Chirurgie; Organ der Deutschsprachigen Arbeitsgemeinschaft fur Handchirurgie; Organ der Deutschsprachigen*, vol. 21, no. 1, pp. 18–22, 1989.

[16] C. R. I. Wheeless, *Arthrodesis of the MP and Finger Joints*, 2012.

[17] J. Craig, *Introduction to Robotics: Mechanics and Control*, ser. Addison-Wesley series in electrical and computer engineering: control engineering. Pearson/Prentice Hall, 2005.

[18] M. Martell and J. Schultz, "Multiport Modeling of Force and Displacement in Elastic Transmissions for Underactuated Hands," *submitted to the IEEE International Conference on Intelligent Robots and Systems*, no. Iros, pp. 1–6, 2014.

[19] Anne M.R. Agur, *Grant's Atlas of Anatomy*. LWW, 2008.

[20] a. M. Hollister, W. L. Buford, L. M. Myers, D. J. Giurintano, and a. Novick, "The axes of rotation of the thumb carpometacarpal joint," *Journal of Orthopaedic Research*, vol. 10, no. 3, pp. 454–460, 1992.

[21] A. Synek, M. Settles, and G. Stillfried, "Multi-body simulation of a human thumb joint by sliding surfaces," *Proceedings of the IEEE RAS and EMBS International Conference on Biomedical Robotics and Biomechatronics*, pp. 379–384, 2012.

[22] J. Garcia de Jalon and E. Bayo, "Multibody Systems with Non-Holonomic Joints," in *Kinematic and Dynamic Simulation of Multibody Systems*. Springer-Verlag, 1994, ch. 3.6, pp. 107–113.

[23] J. M. Cameron and W. J. Book, "Modeling mechanisms with nonholonomic joints using the Boltzmann-Hamel equations," *The International Journal of Robotics Research*, vol. 16, no. 1, pp. 47–59, 1997.

[24] I. M. Bullock, T. Feix, and A. M. Dollar, "Dexterous Workspace of Human Two- and Three-Fingered Precision Manipulation," *IEEE Haptics Symposium*, pp. 41–47, 2014.